

Untuned but not irrelevant: The role of untuned neurons in sensory information coding

Joel Zylberberg^{1,2,3}

¹Department of Physiology and Biophysics, Center for Neuroscience, and Computational Bioscience Program, University of Colorado School of Medicine, Aurora, CO 80045

²Department of Applied Mathematics, University of Colorado, Boulder, CO 80309

³Learning in Machines and Brains Program, Canadian Institute For Advanced Research, Toronto, ON M5G1Z8

September 21, 2017

Abstract

In the sensory systems, most neurons' firing rates are tuned to at least one aspect of the stimulus. Other neurons appear to be untuned, meaning that their firing rates do not depend on the stimulus. Previous work on information coding in neural populations has ignored untuned neurons, based on the tacit assumption that they are unimportant. Recent experimental work has questioned this assumption, showing that in some circumstances, neurons with no apparent stimulus tuning *can* contribute to sensory information coding. These findings are intriguing, because they suggest that – by virtue of our ignoring putatively untuned neurons – our understanding of neural population coding might be incomplete. At the same time, several key questions remain unanswered: Are the impacts of putatively untuned neurons on population coding due to weak tuning that is nevertheless below the threshold the experimenters set for calling neurons tuned (vs untuned)? And why do there appear to be untuned neurons in the brain? Do mixed populations of tuned and untuned neurons have a functional advantage over populations containing only tuned neurons? Using theoretical calculations and analyses of *in vivo* neural data, I answer those questions by: a) showing how untuned neurons can enhance sensory information coding; b) demonstrating that this effect does not rely on weak tuning; and c) identifying conditions under which the neural code can be made more informative by replacing some of the tuned neurons with untuned ones. These conditions specify when there is a functional benefit to having untuned neurons in a circuit, and thus suggest a reason why the brain might contain untuned neurons. Overall, this work shows that, even in the extreme case, where some neurons have *no* tuning, those neurons can still contribute to sensory information coding, and thus should not be ignored.

Introduction

When you look at a picture, signals from your eyes travel along the optic nerve to your brain, where they evoke activity in neurons in the thalamus and visual cortex. As sensory systems neuroscientists, we ask how these patterns of stimulus-evoked brain activity reflect the outside world – in this case, the picture at which you are looking. Other related work asks how patterns of activity in different parts of the brain reflect motor commands

34 sent to the muscles. Answers to these questions are important both for basic science, and for brain-machine
35 interface technologies that either decode brain activity to control prosthetic limbs or other devices [1, 2, 3], or
36 stimulate the brain to alleviate sensory deficits [4, 5].

37 For decades, researchers have addressed these information coding questions by recording neural activity
38 patterns in animals while they are being presented with different stimuli, or performing different motor tasks.
39 That work revealed that many neurons in the relevant brain areas show firing rates that depend systematically
40 on the stimulus presented to the individual, or on the motor task. This neural “tuning” underlies the ability
41 of these neural circuits to encode information about the stimulus and/or behavior. At the same time, many
42 neurons appear to be untuned, thus showing little or no systematic variation in their firing rates as the stimulus
43 (or behavior) is changed [6]. These untuned neurons are typically ignored in studies of neural information
44 coding because it is presumed that they do not contribute [7]. Instead, data collection and analysis are typically
45 restricted to the tuned neurons (for example, consider the selection criteria used by [8, 9]).

46 Recently, researchers have begun to question that assumption: analyses of neural data in the prefrontal
47 cortex [10], somatosensory cortex [11], and auditory cortex (Insanally et al., 2017 cosyne abstract), show that
48 even neurons with no obvious stimulus tuning can nevertheless contribute to the population code. These findings
49 are intriguing, because they suggest that – by virtue of our ignoring the putatively untuned neurons – our
50 understanding of neural population coding might be incomplete. At the same time, several key questions remain
51 unanswered: Are the impacts of putatively untuned neurons on population coding due to weak tuning that is
52 nevertheless below the threshold the experimenters set for calling neurons tuned (vs untuned)? And why do
53 there appear to be untuned neurons in the brain? Do mixed populations of tuned and untuned neurons have a
54 functional advantage over populations containing only tuned neurons?

55 To answer these questions, I used theoretical calculations, and then verified the predictions from those
56 calculations by analyzing 2-photon imaging data collected in the visual cortices of mice that were shown drifting
57 grating stimuli [12]. For the theoretical calculations, I used a common mathematical model of the neural
58 population responses to sensory stimulation [13, 14, 15, 16, 17, 18, 19, 9, 20, 21, 22, 19, 23]. This model describes
59 key features of sensory neural responses: the stimulus tuning (or lack thereof) of individual neurons; the trial-
60 by-trial deviations (or “noise”) in the neural responses [9, 24, 25, 26, 27, 28]; and the potential for that noise to
61 be correlated between neurons [29, 30, 9, 31, 32, 29, 33, 34, 35, 36, 37, 38]. For different conditions – for example,
62 including vs. excluding untuned neurons – I computed the amount of information about the stimulus that is
63 encoded in the population firing patterns. By comparing the information across conditions, I characterized the
64 impact that untuned neurons can have on the neural population code.

65 Because the untuned neurons in the theoretical model have *no* stimulus tuning, these calculations enabled
66 me to demonstrate conclusively that strictly untuned neurons really can contribute to population coding. I
67 provide a geometrical explanation for this phenomenon. Moreover, by studying the information coding of neural
68 populations containing different fractions of tuned vs untuned neurons, I demonstrated that mixed populations
69 can sometimes encode stimulus information better than populations containing only tuned neurons. This provides
70 a functional explanation for why the brain might contain untuned neurons. Using mathematical analyses, I
71 subsequently identified the conditions under which a population code can be made more informative by including
72 some untuned neurons; these analyses explain when untuned neurons enhance brain function. Finally, I used
73 decoding analyses applied to data collected in the visual cortices of awake mice to validate the key predictions
74 of the theory: excluding putatively untuned neurons hinders decoding; and decoding random groups of neurons
75 (both tuned and untuned) yields better performance than does decoding neural populations of the same size,
76 but containing only tuned neurons.

77

Results

78

I first study a theoretical model of information coding in neural populations, to understand whether and how untuned neurons contribute to information coding. I then validate the main predictions from the theory by analyzing data collected in mouse visual cortex.

79

80

81

Theoretical analysis

82

The role of untuned neurons in sensory information coding

83

To investigate the role of untuned neurons in sensory information coding, I studied populations of neurons that encode information about the motion direction of a visual stimulus via their randomly shaped and located tuning curves (Fig. 1A). Many different population sizes were considered. For each population, 70% of the neurons were tuned, and the other 30% were untuned. (These numbers match the fraction of well-tuned neurons selected for analysis in a recent population imaging study [38], and are comparable to the fraction of tuned neurons in the experimental data that I analyzed. I later consider populations with different fractions of untuned neurons.) The untuned neurons had flat tuning curves that did not depend on the stimulus – see the dashed lines in Fig. 1A. The neurons had Poisson-like variability: for each cell, the variance over repeats of a given stimulus was

84

85

86

87

88

89

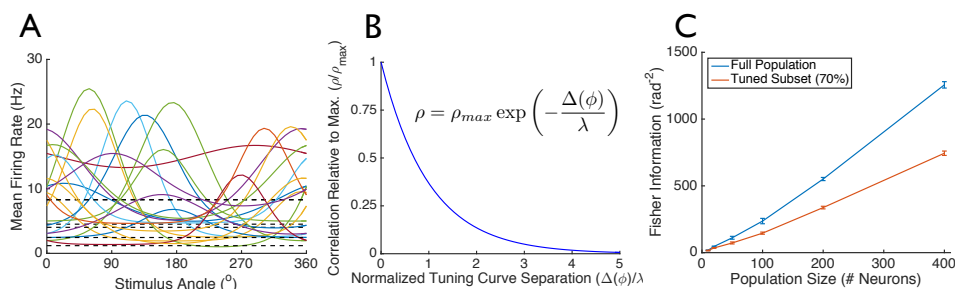


Figure 1: **Untuned neurons can play an important role in sensory information coding.** (A) I considered populations of neurons with randomly shaped and located tuning curves. Of those neurons, 70% were tuned to the stimulus, whereas 30% were untuned – their mean firing rates do not depend on the stimulus (dashed black lines in panel A). The neurons’ trial to trial variability was Poisson-like and correlated between neurons. (B) These correlations followed the “limited-range” structure with $\rho_{max} = 0.75$ and $\lambda = 0.5$ radians (29°). The mean correlation coefficients (averaged over neurons) were 0.12, which is comparable to values reported in primary visual cortex [30]. (Modifying these values did not qualitatively change the results – see Fig. S1). (C) For different sized populations, I computed the Fisher information, which quantifies how well the stimulus can be estimated from the neural population activities. The different lines correspond to: the Fisher information for the full neural populations (blue); and the Fisher information for the tuned 70% of the populations (red). Data points are mean \pm S.E.M., computed over 5 different random draws of the tuning curves.

90

equal to the mean response to that stimulus. This mimics the experimentally observed relation between means and variances of neural activities [25, 23]. The variability was correlated between cells, and the correlation coefficients were chosen to follow the “limited-range” structure reported experimentally [30, 18, 39, 40, 41], and used in previous theoretical studies [13, 14, 15, 20]. With this structure, the correlation coefficients were large for neurons with similar preferred directions, and smaller for neurons with very different preferred directions (see

91

92

93

94

95

96

Methods and Fig. 1B).

97

For each population, I computed the Fisher information (Fig. 1C, blue curve), which quantifies how well an observer – like a downstream neural circuit – can estimate the stimulus direction angle from the neural activities (see Methods). I compared that with the Fisher information obtained from only the tuned subset of neurons – in other words, the information that would be obtained if the untuned cells were ignored (Fig. 1C, red curve). The difference was stark. Ignoring the untuned neurons leads to a dramatic underestimate of the encoded stimulus information. This emphasizes that, despite their lack of stimulus dependence, the untuned neurons can still contribute significantly to the population code.

104

Because the correlation coefficients in Fig. 1 did not depend on the stimulus, it is not the case that the untuned neurons themselves encode information indirectly, through their second-order statistics (as was the case in the theoretical model of [42]). This point is emphasized in Fig. 4, where the information in the population goes to zero as the fraction of untuned neurons approaches 100%. This suggests the question of how untuned neurons contribute to neural information coding. While the untuned neurons’ activities do not reflect the stimulus, they do reflect the trial-specific noise in the tuned neurons’ activities (because they are correlated). Accordingly, a downstream readout – like the circuit receiving these neural spikes – can obtain a less noisy estimate of the stimulus by using the untuned neurons’ activities to estimate the noise in the activities of the tuned neurons, and subtracting that noise estimate from the observed firing rates. Ignoring untuned neurons leads to the loss of the information available through this “de-noising”.

112

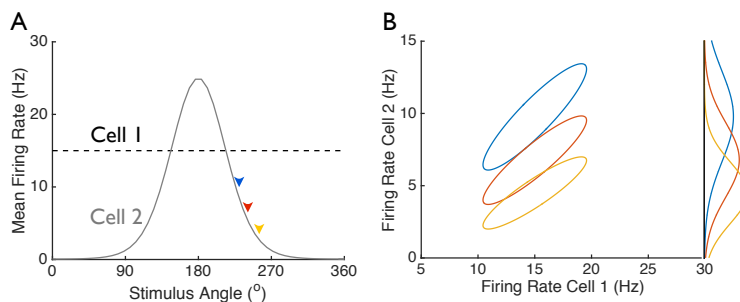


Figure 2: **Untuned neurons can shape noise, improving the population code.** (A) Two neurons’ tuning curves are shown; cell 1 is untuned. In response to stimulation, the cells give noisy responses. That noise is correlated between the two neurons, with a correlation coefficient of 0.9. (B) The distribution of noisy responses to each stimulus is described by an ellipse in the space of the two neurons’ firing rates. The stimulus values are indicated by arrows in panel (A). The ellipses are well separated, meaning that the stimuli can be readily discriminated based on the two cells’ firing rates. If the untuned cell is ignored, then only the tuned cell is observed. The distribution of the tuned cell’s firing rate in response to each stimulus is shown along the right vertical of panel (B). Because those distributions overlap substantially, the stimulus cannot be readily discriminated based only on the firing rate of the tuned cell.

113

114

To illustrate this point, I considered a pair of neurons, one of which is tuned to the stimulus (Fig. 2A). In response to stimulation, the neurons give noisy responses, and that noise is correlated between the two cells. When plotted in the space of the two cells’ firing rates, the distributions of neural responses to each stimulus are defined by ellipses, shown in Fig. 2B. (These are the 1 standard deviation probability contours.) The correlation between cells is reflected in the fact that these ellipses are diagonally oriented. These ellipses are relatively disjoint, meaning that the neural responses to the different stimuli have little overlap, and so it is relatively

115

116

117

118

119

120
121
122
123
124
125
126
127
128
129

unambiguous to infer from the neural firing rates which stimulus was presented. For contrast, consider the neural activities observed when the untuned neuron is ignored. In that case, only the tuned neuron is observed, and the distributions in its responses to the different stimuli overlap substantially (Fig. 2B, right vertical axis). This means that, based on only observations of the tuned cell, the stimulus cannot reliably be determined. Ignoring the untuned neuron leads to a loss of stimulus information. Because the untuned neurons' contribution to the population code relies on their activities reflecting the single-trial noise in the activities of the tuned cells, the untuned neurons do not contribute to population coding if they are independent of the tuned neurons. To demonstrate this point, I repeated the analysis from Fig. 1 (above), but made the untuned neurons uncorrelated from each other and from the tuned neurons. In that case, the untuned neurons do not contribute to the population code: the full population and the tuned subset both have the same amount of stimulus information (Fig. 3A).

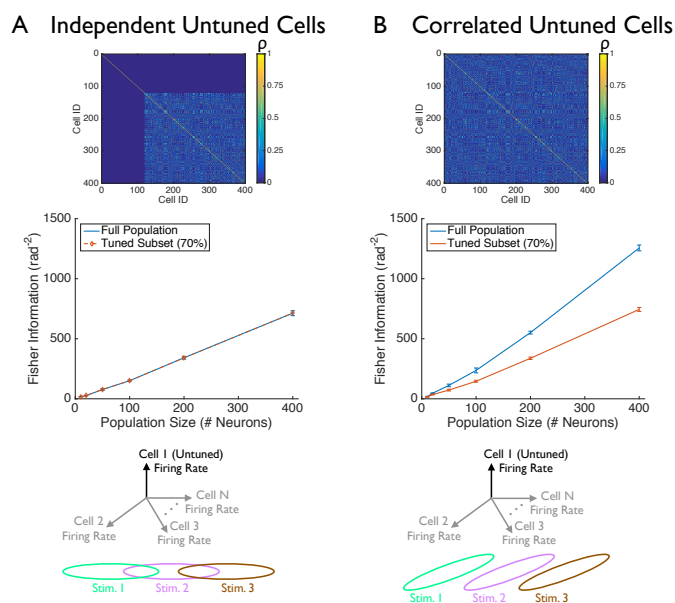


Figure 3: Untuned neurons improve population coding when they are correlated with the tuned neurons. (A) I repeated the analysis from Fig. 1C, and modified it so that the untuned neurons were independent of each other and of the tuned neurons. (B) For comparison, I also show again the results from Fig. 1C. As in Fig. 1, 70% of the neurons in each population were tuned to the stimulus, and 30% were untuned. Upper panels show correlation matrices for 400-cell populations: cells 1 through 120 are untuned, whereas the remainder were tuned. Center panels show the Fisher information for the full neural populations (blue), or for the tuned subsets of neurons in each population (red). (Data points shown are mean \pm S.E.M., computed over 5 different random draws of the tuning curves). The cartoons in the lower panels illustrate why these two different correlation structures lead to untuned neurons having such different effects on the population code (see text). The cartoons show the space of neural firing patterns: each axis is the firing rate of a different neuron. The vertical axis is the firing rate of an untuned neuron. The other axes are the firing rates of tuned cells. Ellipses represent the 1 standard deviation probability contours of the neural population responses to the 3 different stimuli.

130
131

This contribution of untuned neurons to the population code can be understood via the cartoon in Fig. 3B

(lower), which shows the distribution of population responses to 3 different stimuli. In the cartoon, cell 1 is untuned, whereas the rest of the cells are tuned. This means that, as the stimulus changes, the mean responses change along the plane orthogonal to the cell 1 axis. Because the untuned neuron is correlated with the tuned ones, the noise distributions are tilted along the vertical axis. In this configuration, the distributions do not overlap very much. If, however, the untuned neuron is made independent from the tuned ones (as in Fig. 3A), the vertical tilt goes away, causing much more overlap in the response distributions. In other words, when the untuned neurons are correlated with the tuned ones, they improve the population code by separating the responses to different stimuli. This effect disappears when the untuned neurons are independent of the tuned ones.

The results in Figs. 1 and 3 are for neural populations in which information increases without bound as the population size increases. However, in many large neural populations, information saturates with increasing population size [19]. Accordingly, it is important to check that the same results hold for these population codes. As shown in Fig. S2, populations with *information-limiting* correlations, show the same main effect as the populations with limited-range correlations studied in Figs. 1 and 3: ignoring untuned neurons leads to a strong reduction in information.

Mixed populations of tuned and untuned neurons can encode stimulus information more effectively than populations containing only tuned neurons

In the preceding analyses, I showed that neurons with no stimulus tuning can contribute to the population code: ignoring them entails a loss of stimulus information. Here, I turn to the question of why the brain might contain those neurons at all. In other words, is there a functional benefit to including untuned neurons in a population vs having only tuned neurons?

To answer this question, I repeated the analysis from Fig. 1 – again, using populations of heterogeneously tuned neurons with limited-range correlations – but altered the fraction of untuned neurons in each population. The maximum information values were obtained with around 30% of neurons being untuned; this effect was larger in larger populations (Fig. 4A). Because the maximum information does not occur when all of the neurons are tuned (corresponding to an untuned neuron fraction of 0), this analysis shows that neural populations can be made more informative by replacing tuned neurons with untuned ones. This suggests that there may be a functional reason why the brain should contain untuned neurons.

How can mixed populations of tuned and untuned neurons be better at encoding information than populations of the same size but containing only tuned cells? The cartoon in Figs. 4B and C provides some intuition. In both cases, the distributions of firing rates of two neurons are shown, in response to 3 different stimuli (similar to Fig. 2B): ellipses indicate 1 standard-deviation probability contours. In both panels, the neurons have Poisson variability in their firing rates, and the two cells are correlated. In Fig. 4B, both cells are tuned to the stimulus, and the centers of the ellipses are correspondingly displaced relative to each other along both the vertical, and the horizontal, axes of the plot. With this geometrical configuration, the ellipses corresponding to different stimulus-evoked responses overlap substantially: that overlap means that there is ambiguity in determining the stimulus from the neural responses, and so the population code has relatively low information. Fig. 4C differs from Fig. 4B only in the tuning of cell 1: in Fig. 4C, cell 1 is untuned, whereas in Fig. 4B, it was tuned. This means that, in Fig. 4C (where only one of the cells is tuned to the stimulus), the different stimulus-evoked response distributions are displaced relative to each other only in the vertical direction, and not the horizontal one. Owing to the diagonal orientation of the ellipses, there is less overlap between the different response distributions in Fig. 4C than 4B. Consequently, the pair of neurons in Fig. 4C (one of which is untuned) is better at encoding stimulus information than the pair of neurons in Fig. 4B (both of which are tuned to the stimulus).

The cartoon in Figs. 4BC shows how the presence of untuned neurons can improve the population code:

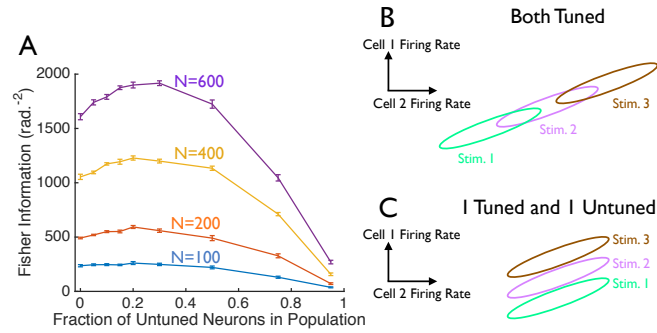


Figure 4: Populations containing some untuned neurons can encode more information than ones with only tuned neurons. (A) I repeated the calculations from Fig. 1, but with different fractions of untuned neurons in each population. For several different population sizes (indicated on the plot), the Fisher information is shown as a function of the fraction of untuned neurons in the population. As in Fig. 1, each population had limited-range correlations, with average correlation coefficients that are in the physiological range. Error bars are the S.E.M. over 5 random sets of different tuning curves. (B and C) Cartoon showing how mixed populations containing tuned and untuned neurons can be better at encoding information than populations containing only tuned neurons. In response to 3 different stimuli, I show the 1 standard-deviation probability contours in the responses of a pair of neurons. In all cases, the neurons have Poisson variability, and correlated noise. In panel (B), both cells are tuned to the stimulus, whereas in panel (C), cell 2 is tuned to the stimulus, and cell 1 is untuned.

176 including untuned neurons modifies the *signal correlation* structure (the correlation between neurons in the
 177 stimulus-evoked mean responses) relative to the case where both neurons are tuned. And because the relationship
 178 between the signal and noise correlations determines the population coding efficacy [17, 16, 14], this modification
 179 can improve the population code overall.

180 Under what conditions do mixed populations contained tuned and untuned neurons encode stimulus infor-
 181 mation better than populations containing only tuned cells? To answer this question, I performed mathematical
 182 analyses – described in detail in the Methods – that identify conditions where the population code can be made
 183 more informative by replacing a tuned neuron (neuron k) by an untuned one. Those analyses showed that
 184 making neuron k untuned will improve the population code whenever the following inequality holds:

$$-2 \frac{df_k}{ds} \sum_{j \neq k} C_{kj}^{-1} \frac{df_j}{ds} > \left(\frac{df_k}{ds} \right)^2 C_{kk}^{-1}, \quad (1)$$

185 where $\frac{df_k}{ds}$ is the slope of the tuning curve of neuron k , and C is the covariance matrix of the neural variability.
 186 Intuitively, this equation compares the loss of information from removing the tuning of neuron k (the right-hand
 187 side of Eq. 1), with the gain in information from the noise-shaping effect shown in Figs. 4BC (the left-hand
 188 side of Eq. 1). Whenever the gain exceeds the loss, it is beneficial to make neuron k untuned. Note that the
 189 inequality in Eq. 1 will not necessarily be satisfied by all sets of neural tuning curves and covariance matrices.
 190 Consequently, it is not guaranteed that including untuned neurons will *always* improve the population code.
 191 However, under the condition specified by Eq. 1, there is a functional benefit to including untuned neurons in a
 192 population.

193 **Analysis of *in vivo* neural activities**

194 The theoretical work described above makes a key prediction: the ability to decode a stimulus from the evoked
 195 neural population activities could be improved if untuned neurons are included in those populations, as opposed
 196 to being ignored. To test this prediction, I analyzed data from 2-photon Ca^{2+} imaging recordings done in primary
 197 visual cortex of awake mice (data from [12]) whose neurons expressed the genetically encoded calcium indicator
 198 GCaMP6f. The mice were presented with stimuli consisting of gratings drifting in 8 different directions, and
 199 the fluorescence levels of $\mathcal{O}(100)$ neurons were observed in each experiment. I analyzed the data from 46 such
 200 experiments.

201 For each stimulus presentation and neuron, I extracted the mean fluorescence change during the stimulus
 202 presentation, relative to the fluorescence in the period before the stimulus presentation: this $\Delta F/F$ value mea-
 203 sures the stimulus-induced change in neural activity. I then computed the neurons’ tuning curves by averaging
 204 these $\Delta F/F$ values over all trials in which the stimulus drifted in each direction. Some of the neurons had well-
 205 defined direction tuning curves (Fig. 5A), whereas others were relatively untuned (Fig. 5B). Following [43, 9], I
 206 categorized these cells as tuned or putatively untuned (hereafter referred to simply as *untuned*) based on their
 207 direction selectivity indices (see Methods). Between the 46 experiments, $5379/8943 \approx 60\%$ of the neurons were
 208 classified as being tuned for direction. (In the population coding analyses discussed below, I consider several
 different thresholds for labelling neurons as “tuned” vs “untuned”.)

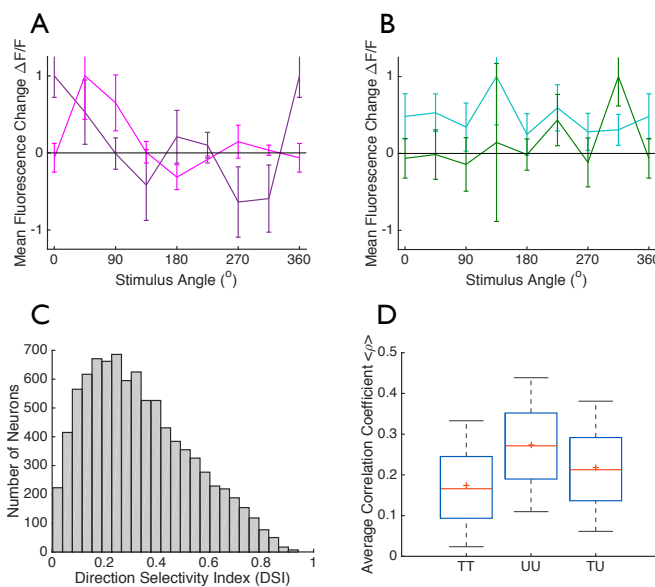


Figure 5: **Tuned and untuned neurons are correlated *in vivo*.** Neurons’ responses to drifting grating stimuli were measured using 2-photon Ca^{2+} imaging. (A) Tuning curves for two direction tuned neurons. (B) Tuning curves of two untuned neurons. Markers show mean $\Delta F/F \pm$ S.E.M, calculated over 75 trials of each stimulus direction. (C) Direction selectivity indices for the 8493 neurons whose stimulus-evoked responses were measured. (D) The distributions of correlation coefficients for cell pairs of different types: where both cells were direction tuned (“TT”; $n = 391833$ pairs); where both cells were untuned (“UU”; $n = 150801$ pairs); and where one cell was tuned and one was untuned (“TU”; $n = 434752$ pairs). Each box plot shows the median, the range (maximum and minimum indicated by black bars), and the boundaries of the 25th and 75th percentiles (blue box) of the distributions.

210
211
212
213
214
215
216
217
218
219
220
221
222

Along with the tuning, I measured the correlations in the cells' trial-to-trial variability over repeats of each stimulus. These "noise correlations" are shown all pairs of simultaneously observed neurons (Fig. 5D). The correlation coefficients were typically positive for pairs of tuned neurons ("TT"), pairs of untuned neurons ("UU"), and mixed pairs consisting of one tuned and one untuned neuron ("TU"). Because there were correlations between the tuned and untuned neurons, the theory predicts that stimulus decoding could be improved by including the untuned neurons, as opposed to ignoring them.

To test this prediction, I used the logistic regression method of [44] to take in vectors of neural activity recorded in response to one of 2 different stimuli, and to identify the stimulus from those neural responses (see Methods for details). I then computed the fraction of trials on which the stimulus was correctly identified.

I first performed this analysis on the full populations of recorded neurons – including the tuned and untuned ones – and compared this to the decoding performance when only tuned neurons were used by the decoder. Using all of the neurons resulted in $10 \pm 1\%$ (mean \pm S.E.M) better decoding performance ($p = 8.9 \times 10^{-11}$, paired one-sided t-test; and $p < 10^{-8}$, non-parametric binomial test of significance) than did using only the tuned neurons (Fig. 6A).

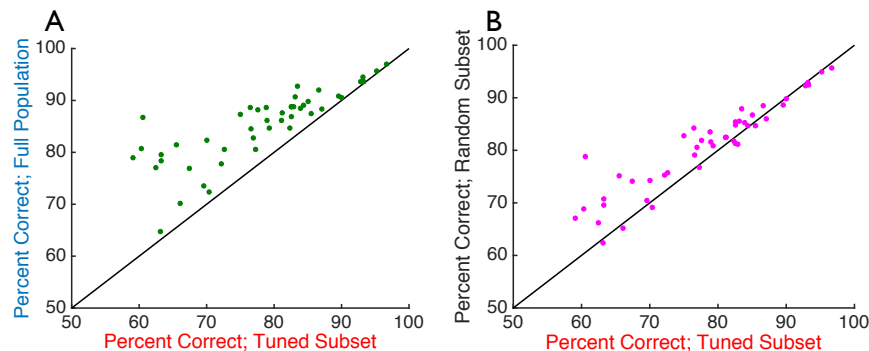


Figure 6: **Untuned neurons can enhance information coding in *in vivo* neural populations.**

I used logistic regression to perform pairwise discrimination on the population response vectors, to determine which of 2 different stimuli caused each response. I repeated this analysis for all possible pairs of stimuli: reported values are the percentage of trials for which the stimulus was correctly identified, averaged over all possible pairings (there is one data point per experiment). (A) Decoding accuracy when the full population response vectors were decoded (vertical axis) vs. when only the tuned subsets of the neurons are seen by the decoder (horizontal axis). (B) Decoding accuracy when random subsets of the neurons (of the same size as the tuned subset, but containing both tuned and untuned neurons) are input to the decoder (vertical axis) vs. when only the tuned subsets of the neurons are seen by the decoder (horizontal axis). Chance performance for this binary discrimination task is 50%. Diagonal line denotes equality.

223
224
225
226
227
228
229
230

Next, I asked whether – as in the theoretical calculations in Fig. 4 – populations that include both tuned and untuned neurons could yield better decoding vs populations of the same size but containing only tuned cells. To answer this question, I extracted a random subset of the neurons from each population, that was the same size as the set of tuned neurons within that population. I then performed the logistic regression analysis on these random subsets, and compared the performance with that which was obtained on the tuned subsets (Fig. 6B). On average, the decoding performance was $4 \pm 1\%$ (mean \pm S.E.M.) better using the random subsets vs the fully tuned ones, a modest but statistically significant difference ($p = 1.7 \times 10^{-5}$, paired single-sided t-test; and

231 $p = 0.027$, non-parametric binomial test of significance).

232 It is important to check that the results in Fig. 6 do not depend on the specific criterion used to distinguish
233 tuned from putatively untuned neurons. Consequently, I repeated the analysis from Fig. 6 with several different
234 criteria (see Methods and Figs. S3-S4). These results are all in qualitative agreement with those of Fig. 6:
235 regardless of the specific criterion that is used, the putatively untuned neurons contribute to the population
236 code, and mixed populations of tuned and untuned neurons encode more information than do populations of the
237 same size but containing only tuned neurons.

238 Discussion

239 I showed that, when the variability in neural responses to stimulation is correlated between cells, even neurons
240 whose firing rates do not depend on the stimulus (“untuned” neurons) can contribute to sensory information
241 coding. Moreover, in at least some cases, populations with both tuned and untuned neurons can convey more
242 information about the stimulus than do populations of the same size but containing only tuned neurons. These
243 effects were observed in both a theoretical model (Figs. 1-4), in and in large population recordings from mouse
244 visual cortex (Fig. 6). These experimental findings were not sensitive to the specific criterion used to define
245 neurons as being tuned vs untuned (Figs. S3-S4).

246 These results have two main implications. First, our understanding of how the sensory systems encode
247 information about the outside world is likely to be incomplete unless it includes the contributions of all neurons,
248 regardless of whether or not they appear to be tuned to the stimulus. This means that current practices, in
249 which putatively untuned neurons are ignored during data collection and analysis, might be hindering progress.
250 Moreover, because there is not always a clear distinction between tuned and untuned neurons (Fig. 5C: histogram
251 is unimodal) – and this effect is confounded by noise in the experimental measurements – selection criteria are
252 largely arbitrary. This experimental noise also means that it is nearly impossible to know whether there really
253 are strictly “untuned” (as opposed to only weakly tuned) neurons in the brain. Either way, the results shown
254 here suggest that, rather than discarding neurons with weak (or zero) tuning, it is better to simply include all
255 the neurons in the analysis: even in the extreme case, where those neurons really have *no* tuning, they can still
256 contribute to the population code. This last point applies especially to decoding population activities to control
257 brain-machine interface devices: better performance could be obtained by decoding all neurons, as opposed to
258 decoding only the well-tuned ones (Fig. 6A).

259 Second, because adding untuned neurons can increase the stimulus information (Figs. 4, 6B), there might be
260 a functional benefit to having some untuned neurons in a population. This is related to previous observations
261 that heterogeneous tuning curves could confer advantages on the population code [45, 15]. Those previous studies
262 did not, however, consider the role of untuned neurons in the population code. Here, I showed the conditions
263 under which mixed populations containing tuned and untuned neurons can better encode the stimulus than
264 can populations of the same size (and same level of neural variability), but containing only tuned cells. It is
265 important to note, however, that no brain area can encode more stimulus information than it received from its
266 inputs [46, 23]. This is the *data-processing inequality*, and it implies that there is not a limitless increase in
267 information to be obtained by adding large numbers of untuned neurons to neural circuits.

268 Observations related to those presented here have also been made by Insanally and colleagues (Cosyne 2017
269 abstract), and by [10, 11] based on analyses of *in vivo* neural data. There, as in the analysis of mouse data
270 presented here, it is hard to distinguish weakly tuned neurons from purely untuned ones, and thus difficult to
271 isolate the coding benefits of putatively untuned neurons due to noise shaping, vs those due to non-zero tuning,
272 that is nonetheless under the chosen threshold. (However, the fact that the results are not sensitive to the
273 specific criterion used to label neurons as tuned vs untuned does help to make this distinction: Figs. S3, S4).

274 This complication highlights the value of the theoretical work presented here (Figs. 1-4): in the model, the
275 untuned neurons really have no stimulus dependence, enabling us to shown that even neurons with *no* tuning
276 can contribute to sensory information coding.

277 For large neural populations, an astronomically large number of different correlation patterns are possible
278 (and this problem is confounded when one includes correlations of higher order than the pairwise ones considered
279 here [47, 48]). Accordingly, it was not possible to simulate all possible correlation patterns in the theoretical
280 study. Thus, it is natural to ask how general the results are over different correlation structures. Here, the fact
281 that I saw consistent effects in the experimental data (Fig. 6) as in the theoretical model with limited range
282 correlations (Fig. 1), and the model with information-limiting correlations (Fig. S2), argues for the generality
283 and applicability of the findings.

284 The experimental data studied here (Figs. 5 and 6) were recorded while mice were passively viewing the
285 visual stimulus. Consequently, the correlated fluctuations in visual cortical neural activity could correspond
286 to changes in attention, arousal, or other factors that were not controlled in the experiment. As a result, it
287 is important for future work to assess the role of untuned neurons under experimental conditions with more
288 carefully controlled behavior; that work is beyond the scope of this study.

289 Adding neurons to a population can never decrease the amount of encoded stimulus information: because
290 a downstream read-out could always choose to ignore the added cells, those cells can at worst contribute zero
291 information. Consequently, untuned neurons can never *hinder* the population code. (However, decoding based
292 on observations with small numbers of trials is subject to overfitting. In this case, adding more cells can hinder
293 the decoding because the decoder might be inaccurate). This means that the potential effects of untuned neurons
294 on population coding range between no contribution (Fig. 3A), and positive contributions at least as large as
295 those seen in Fig. 1C (i.e., at least 70% increase in information available by including vs. ignoring untuned
296 neurons). There may be other cases in which the positive contributions of untuned neurons are even larger.

297 It is important not to interpret the results presented here as implying that neural tuning is not essential to
298 sensory information coding. Whereas the theoretical model of [42] can encode stimulus information via changes
299 in the correlations between neurons, that effect is not responsible for the results shown here. Notably, for the
300 theoretical calculations in Figs. 1-4, the correlations do not depend on the stimulus, yet nevertheless the untuned
301 neurons contribute to the population code. Underscoring this point is the fact that, if there are no tuned neurons
302 in our models, there is no stimulus information (Fig. 4: information approaches zero as the fraction of untuned
303 neurons approaches 1). Moreover, the fact that a quasi-linear decoder can identify the stimuli presented to the
304 mouse, based on the visual cortical activity patterns (Fig. 6), suggests that the information is being encoded in
305 the firing rates and not the correlation patterns. Given that this neurally plausible decoder [44] would not be
306 able to extract information that depended only on the stimulus-dependence of the correlations between neurons,
307 this is an important distinction.

308 We conclude by noting that, even when untuned neurons do not by themselves encode information about the
309 stimulus, they can shape the noise in the population responses, thereby improving the population code overall.
310 Thus, untuned neurons are not irrelevant for sensory information coding.

311 Methods

312 I first discuss the theoretical calculations, and then the analysis of experimental data.

313

Theoretical Calculations

314

Modeling the stimulus-evoked neural responses, and the information encoded

315

I considered for simplicity a 1-dimensional stimulus s (for example, the direction of motion of a drifting grating).

316

In response to the stimulus presentation, the neural population displays firing rates \vec{r}_i , where the index i denotes

317

the trial. (Each element of the vector \vec{r}_i is the firing rate of a single neuron). These responses have two

318

components. The first, $\vec{f}(s)$, is the mean (trial-averaged) response to stimulus s , whereas the second component,

319

$\vec{\epsilon}_i$, represents the trial-by-trial fluctuations, or “noise” in the neural firing rates.

$$\vec{r}_i = \vec{f}(s) + \vec{\epsilon}_i \quad (2)$$

320

The tuning curves were chosen to be either Von Mises functions (as in [15, 17, 23]), or, in the case of untuned

321

neurons, to be constants (Fig. 1A). The parameters of the tuning curves were randomly drawn, using the same

322

distributions as in [23].

323

The neurons’ noise variances were chosen to match the mean responses, in accordance with experimental

324

observations of Poisson-like variability. I considered different patterns of inter-neural correlation, as described

325

below.

326

For each set of tuning curves and correlations, I used the typical linear Fisher information measure, $I(s)$, to

327

quantify the ability of downstream circuits to determine the stimulus, s , from the noisy neural responses on each

328

trial \vec{r}_i [13, 14, 15, 16, 17, 18, 20, 22, 19, 21, 23]:

$$I(s) = \vec{f}'^T(s) [C(s)]^{-1} \vec{f}'(s), \quad (3)$$

329

where the prime denotes a derivative with respect to the stimulus, the superscript T denotes the transpose

330

operation, and $C(s) = \text{cov}(\vec{\epsilon}_i | s)$ is the covariance matrix of the noise in the neural responses to stimulus s . For

331

all calculations, I checked that the correlation (and covariance) matrices were positive semi-definite (thus being

332

physically realizable) before performing the Fisher information calculations.

333

To compute the information for a subset of a neural population, I extracted the block of the covariance

334

matrix, and the elements of the vector $\vec{f}'(s)$, that correspond to the neurons in that subset. I then used those

335

values in Eq. 2.

336

For all of the information values presented here, I computed the information for each of 50 different stimulus

337

values, evenly spaced over $[0^\circ, 360^\circ]$. The reported values are averages over these 50 stimuli. This accounts for

338

the fact that Fisher information $I(s)$ is a *local* quantity which varies from stimulus to stimulus. By averaging

339

over many stimuli, I avoid the possibility that the reported information values might be atypical, and affected

340

by the specific stimulus at which the information was calculated.

341

Limited-range correlations

342

The elements of covariance matrix $C(s)$ were $C_{ij}(s) = \sqrt{f_i(s)f_j(s)}\rho_{ij}$, where ρ_{ij} is the correlation between cells

343

i and j . The factor of $\sqrt{f_i(s)f_j(s)}$ ensures that the neurons have Poisson variability (variance of noise is equal

344

to mean firing rate, meaning that standard deviation of noise is equal to square root of mean firing rate).

345

The correlation coefficients ρ_{ij} were calculated from the equation in Fig. 1B. The tuning curve separation

346

$\Delta(\phi)$ for each cell pair was computed as $\Delta(\phi) = |\arccos[\cos(\phi_i - \phi_j)]|$, where ϕ_i and ϕ_j are the cells’ preferred

347

direction angles (the locations of their tuning curve peaks). This formula accounts for the fact that angles “wrap”

348

around the circle: so values of 10° and 350° have a separation of 20° (and not 340°).

349

For the untuned neurons, their preferred stimulus angles were randomly assigned, uniformly over the range

350

$[0^\circ, 360^\circ]$.

When do untuned neurons improve population coding?

Here, I derive Eq. 1 from the main text, which specifies the conditions under which including untuned neurons in a population improves its ability to encode stimulus information. To do this, I compute the information in the neural population, and the information that would be obtained if one of the neurons were to be made untuned. I then ask when the information increases as a result of this change.

I start by considering the linear Fisher information (Eq. 3), and explicitly describe the summation over neurons:

$$I(s) = \sum_{ij} f'_i(s) f'_j(s) C_{ij}^{-1}(s), \quad (4)$$

where the prime denotes a derivative with respect to the stimulus, and $C(s) = \text{cov}(\vec{\epsilon}_i | s)$ is the covariance matrix of the noise in the neural responses to stimulus s .

If neuron k were to be replaced by an untuned neuron, $f'_k(s)$ would be set to zero, and the population would now have a Fisher information value of

$$\begin{aligned} \tilde{I}(s) &= \sum_{ij} f'_i(s) (1 - \delta_{ik}) f'_j(s) (1 - \delta_{jk}) C_{ij}^{-1}(s) \\ &= I(s) - 2f'_k(s) \sum_j C_{kj}^{-1}(s) f'_j(s) + (f'_k(s))^2 C_{kk}^{-1}(s) \\ &= I(s) - (f'_k(s))^2 C_{kk}^{-1}(s) - 2f'_k(s) \sum_{j \neq k} C_{kj}^{-1}(s) f'_j(s), \end{aligned} \quad (5)$$

where δ_{ij} is the Kronecker delta (equal to 1 if $i = j$, and zero otherwise), and $I(s)$ the Fisher information value from Eq. 4.

Whenever $\tilde{I}(s) > I(s)$, the population code is made more informative by the inclusion of an untuned neuron. That condition corresponds to

$$-2f'_k(s) \sum_{j \neq k} C_{kj}^{-1}(s) f'_j(s) > (f'_k(s))^2 C_{kk}^{-1}(s), \quad (6)$$

which is Eq. 1 of the main text.

Analysis of *in vivo* neural recordings

Overview of the experiment

The full description of the experiment is given by [12], and so I briefly summarize here. GCaMP6f was expressed in the excitatory neurons of the forebrain of mice. 2-photon imaging was used to measure the fluorescence of neurons in visual cortex through a cranial window. The mice were presented with drifting grating stimuli. The stimuli could move in any of 8 different directions, and at 6 different temporal frequencies. The stimuli were presented for 2 seconds each, followed by a 1 second gray screen before the next stimulus was presented. Each combination of direction and frequency was presented repeatedly (either 15 or 30 times each, depending on the temporal frequency).

Data access

Following the example Jupyter notebook provided by [12] – which provides a template for accessing the experimental data – I retrieved the following data: average $\Delta F/F$ values for each neuron on each trial, and the stimulus direction for each trial. I analyzed all of the neurons observed in each experiment, and not only those that were labelled as visually responsive.

381

Tuning curves

382

I calculated the tuning curves (Figs. 5A and B) by averaging the $\Delta F/F$ values for all trials of each direction: this *marginalizes* over the different temporal frequencies. The noise correlations coefficients (Fig. 5D) were computed over repeats of the same stimulus (same orientation and temporal frequency), and then averaged over all stimuli.

385

386

Statistical tests of significance

387

For the results in Figs. 6, S3, and S4, I used two different methods to assess statistical significance. First, I used the standard paired sample t-tests. Second, I used non-parametric tests described below. These are typically more conservative because they are not sensitive to non-Gaussianity in the data. Both methods showed that the experimental results are significant.

390

391

For the non-parametric tests, I identified the number, K , of experiments in which the effect was positive. For example, for Fig. 6A, this was the number of experiments in which the full population gave better decoding performance than did the subset containing only tuned neurons. I then computed the probability that, of the $N = 46$ experiments, K or more of them would have a positive effect, if the outcome of each experiment came from an unbiased coin flip (which assigned a positive, or negative, effect with equal probability). This probability is obtained from the binomial distribution, and gives the probability that we would have observed the same results by random chance.

396

397

398

Identifying tuned vs untuned neurons

399

Following [43, 9], direction selective cells were identified via their *circular variance*, with the direction selectivity index (DSI) computed for each neuron as follows. For each stimulus direction, I computed the two-dimensional direction vector $d(\theta) = [\cos(\theta), \sin(\theta)]$, and multiplied that by the neuron's mean response to this stimulus $r(\theta)$ (i.e., the tuning curve value for that stimulus). This yielded a vector $v(\theta) = r(\theta)d(\theta)$ that points in the direction of the stimulus, with the length determined by the cell's mean response to the stimulus. I then averaged this vector over all stimulus directions. If the neuron gave equal responses to all stimuli, the horizontal and vertical components of $v(\theta)$ would average out to zero over all the stimuli, whereas if the neuron responds selectively to one stimulus direction, this cancellation would not occur. Consequently, the DSI is measured by the length of $\langle v(\theta) \rangle$, relative to the neuron's mean response (averaged over all stimuli):

407

$$DSI = \frac{|\langle v(\theta) \rangle|}{\langle r(\theta) \rangle}. \quad (7)$$

408

If the neuron responds strongly to only one stimulus direction, the DSI can be as large as 1, and the DSI can be as small as 0 for neurons that respond equally to all stimuli.

409

410

To identify tuned (vs “untuned”) neurons, I chose a cutoff of $DSI > 0.25$. This matches the smallest DSI of the direction-selective retinal ganglion cells studied by [9]. I also repeated the decoding analysis from Fig. 6 with different cutoffs on the DSI, and found qualitatively similar results: the precise value of the cutoff is unimportant (Figs. S3 and S4).

413

414

Logistic regression decoding analysis

415

I used the logistic regression method of [44]. The classifier was trained to take in vectors of neural responses, in response to two different stimuli, and to return labels (“0” or “1”) that indicate which of the two stimuli was presented on each trial. I randomly divided the data into a training set (75% of the data) that was used to fit the weights of the classifier, and a test set (25% of the data) that was used to measure the performance. After

418

419 training on the training data, I applied the classifier to the neural responses from the test data set, yielding
420 an output value for each response vector. Values above 0.5 indicated that the stimulus was most likely to be
421 stimulus “1”, whereas values less than 0.5 were taken to indicate that response was most likely generated by
422 stimulus “0”. I then computed the fraction of these test trials on which this classifier correctly identified the
423 stimulus that caused the neural response. This analysis was separately done for all $(8 \times 7)/2 = 28$ different
424 stimulus pairings: reported performance values are averages over all such stimulus pairings.

425 Acknowledgments

426 Thanks to Eric Shea-Brown and Alex Cayco-Gajic for helpful discussions, and to the Allen Institute for sharing
427 their *in vivo* datasets. JZ gratefully acknowledges the following funding: Canadian Institute for Advanced
428 Research (CIFAR) Azrieli Global Scholar Award, Sloan Research Fellowship, and Google Faculty Research
429 Award.

430 References

- 431 [1] Lebedev MA, Nicolelis MA (2006) Brain-machine interfaces: past, present and future. *Trends Neurosci* 29:
432 536–546.
- 433 [2] Santhanam G, Ryu SI, Byron MY, Afshar A, Shenoy KV (2006) A high-performance brain-computer
434 interface. *Nature* 442: 195–198.
- 435 [3] Sadtler PT, Quick KM, Golub MD, Chase SM, Ryu SI, et al. (2014) Neural constraints on learning. *Nature*
436 512: 423–426.
- 437 [4] Bensmaia SJ (2015) Biological and bionic hands: natural neural coding and artificial perception. *Phil Trans*
438 *R Soc B* 370: 20140209.
- 439 [5] Delhaye BP, Saal HP, Bensmaia SJ (2016) Key considerations in designing a somatosensory neuroprosthesis.
440 *J Physiol - Paris* (in press) .
- 441 [6] Ringach DL, Shapley RM, Hawken MJ (2002) Orientation selectivity in macaque v1: diversity and laminar
442 dependence. *J Neurosci* 22: 5639–5651.
- 443 [7] Olshausen BA, Field D (2006) What is the other 85 percent of v1 doing? In: van Hemmen L, Sejnowski T,
444 editors, *Problems in Systems Neuroscience*, Oxford Press. pp. 182–211.
- 445 [8] Graf A, Kohn A, Jazayeri M, Movshon J (2011) Decoding the activity of neuronal populations in macaque
446 primary visual cortex. *Nat Neurosci* 14: 239–245.
- 447 [9] Zylberberg J, Cafaro J, Turner M, Shea-Brown E, Rieke F (2016) Direction-selective circuits shape noise
448 to ensure a precise population code. *Neuron* (89): 369–383.
- 449 [10] Leavitt ML, Pieper F, Sachs AJ, Martinez-Trujillo JC (2017) Correlated variability modifies working mem-
450 ory fidelity in primate prefrontal neuronal ensembles. *Proc Natl Acad Sci USA* 114: E2494–E2503.
- 451 [11] Safaai H, von Heimendahl M, Sorando JM, Diamond ME, Maravall M (2013) Coordinated population
452 activity underlying texture discrimination in rat barrel cortex. *J Neurosci* 33: 5843–5855.
- 453 [12] Allen Brain Observatory (2016). <http://observatory.brain-map.org/visualcoding/>. Accessed: 2017-
454 04-17.
- 455 [13] Abbott LF, Dayan P (1999) The effect of correlated variability on the accuracy of a population code. *Neural*
456 *Comput* 11: 91–101.

- 457 [14] Averbeck BB, Latham PE, Pouget A (2006) Neural correlations, population coding and computation. *Nat*
458 *Rev Neurosci* 7: 358–366.
- 459 [15] Ecker AS, Berens P, Tolias AS, Bethge M (2011) The Effect of Noise Correlations in Populations of Diversely
460 Tuned Neurons. *J Neurosci* 31: 14272–14283.
- 461 [16] da Silveira RA, Berry MJ (2014) High-Fidelity Coding with Correlated Neurons. *PLoS Comput Biol* 10:
462 e1003970.
- 463 [17] Hu Y, Zylberberg J, Shea-Brown E (2014) The sign rule and beyond: Boundary effects, flexibility, and noise
464 correlations in neural population codes. *PLoS Comput Biol* 10: e1003469.
- 465 [18] Shamir M (2014) Emerging principles of population coding: in search for the neural code. *Curr Opin*
466 *Neurobiol* 25: 140-148.
- 467 [19] Moreno-Bote R, Beck J, Kanitscheider I, Pitkow X, Latham P, et al. (2014) Information-limiting correlations.
468 *Nat Neurosci* 17: 1410-1417.
- 469 [20] Sompolinsky H, Yoon H, Kang K, Shamir M (2001) Population coding in neuronal systems with correlated
470 noise. *Phys Rev E* 64: 051904.
- 471 [21] Averbeck BB, Lee D (2006) Effects of noise correlations on information encoding and decoding. *J Neurophys*
472 95: 3633–3644.
- 473 [22] Josić K, Shea-Brown E, Doiron B, de la Rocha J (2009) Stimulus-dependent correlations and population
474 codes. *Neural Comput* 21: 2774–2804.
- 475 [23] Zylberberg J, Pouget A, Latham P, Shea-Brown E (2017) Robust information propagation through noisy
476 neural circuits. *PLoS Comput Biol* 13: e1005497.
- 477 [24] Britten K, Shadlen M, Newsome W, Movshon J (1993) Responses of neurons in macaque MT to stochastic
478 motion signals. *Visual Neurosci* 10: 1157-1169.
- 479 [25] Churchland M, Yu B, Cunningham J, Sugrue L, Cohen M, et al. (2010) Stimulus onset quenches neural
480 variability: a widespread cortical phenomenon. *Nat Neurosci* 13: 369-378.
- 481 [26] Franke F, Fiscella M, Sevelev M, Roska B, Hierlemann A, et al. (2016) Structure of neural correlation and
482 how they favor coding. *Neuron* 89: 409-422.
- 483 [27] Zylberberg J, Hyde R, Strowbridge B (2016) Dynamics of robust pattern separability in the hippocampal
484 dentate gyrus. *Hippocampus* (29): 623-632.
- 485 [28] Faisal A, Selen L, Wolpert D (2008) Noise in the nervous system. *Nat Rev Neurosci* 9: 292-303.
- 486 [29] Zohary E, Shadlen MN, Newsome WT (1994) Correlated neuronal discharge rate and its implications for
487 psychophysical performance. *Nature* 370: 140–143.
- 488 [30] Cohen MR, Kohn A (2011) Measuring and interpreting neuronal correlations. *Nat Neurosci* 14: 811–819.
- 489 [31] Lampl I, Reichova I, Ferster D (1999) Synchronous membrane potential fluctuations in neurons of the cat
490 visual cortex. *Neuron* 22: 361-374.
- 491 [32] Alonso J, Usrey W, Reid R (1996) Precisely correlated firing of cells in the lateral geniculate nucleus. *Nature*
492 383: 815–819.
- 493 [33] Goris R, Movshon J, Simoncelli E (2014) Partitioning neuronal variability. *Nat Neurosci* 17: 858-865.
- 494 [34] Smith M, Kohn A (2008) Spatial and temporal scales of neuronal correlation in primary visual cortex. *J*
495 *Neurosci* 28: 12591-12603.
- 496 [35] Ecker A, et al (2014) State dependence of noise correlations in macaque primary visual cortex. *Neuron* 82:
497 235-248.

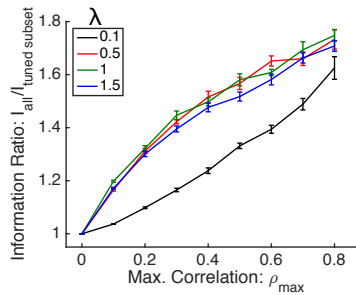
- 498 [36] Scholvinck M, Saleem A, Benucci A, Harris K, Carandini M (2015) Cortical state determines global vari-
499 ability and correlations in visual cortex. *J Neurosci* 35: 170-178.
- 500 [37] Lin IC, Okun M, Carandini M, Harris K (2015) The nature of shared cortical variability. *Neuron* 87:
501 644-656.
- 502 [38] Montijn JS, Meijer GT, Lansink CS, Pennartz CM (2016) Population-level neural codes are robust to
503 single-neuron variability from a multidimensional coding perspective. *Cell Rep* 16: 2486-2498.
- 504 [39] Bair W, Zohary E, Newsome WT (2001) Correlated firing in macaque visual area MT: time scales and
505 relationship to behavior. *J Neurosci* 21: 1676-1697.
- 506 [40] Reich DS, Mechler F, Victor JD (2001) Independent and redundant information in nearby cortical neurons.
507 *Science* 294: 2566-2568.
- 508 [41] Gawne TJ, Richmond BJ (1993) How independent are the messages carried by adjacent inferior temporal
509 cortical neurons? *J Neurosci* 13: 2758-2771.
- 510 [42] Burge J, Geisler WS (2015) Optimal speed estimation in natural image movies predicts human performance.
511 *Nat Comm* 6.
- 512 [43] Mazurek M, Kager M, Van Hooser SD (2014) Robust quantification of orientation selectivity and direction
513 selectivity. *Frontiers Neural Circuits* 8: 92.
- 514 [44] Berens P, Ecker A, Cotton R, Ma W, Bethge M, et al. (2012) A fast and simple population code for
515 orientation in primate v1. *J Neurosci* 32: 10618-10626.
- 516 [45] Shamir M, Sompolinsky H (2006) Implications of neuronal diversity on population coding. *Neural Comput*
517 18: 1951-1986.
- 518 [46] Beck JM, Ma W, Pitkow X, Latham PE, Pouget A (2012) Not noisy, just wrong: the role of suboptimal
519 inference in behavioral variability. *Neuron* 74: 30-39.
- 520 [47] Zylberberg J, Shea-Brown E (2015) Input nonlinearities can shape beyond-pairwise correlations and improve
521 information transmission by neural populations. *Phys Rev E* 92: 062707.
- 522 [48] Cayco-Gajic A, Zylberberg J, Shea-Brown E (2015) Triplet correlations among similarly-tuned cells impact
523 population coding. *Front Comput Neurosci* 9: 57.

524

Supplemental Information and Figures

525

Figure S1: different parameters for the limited-range correlations



Supplementary Figure 1: **Dependence of information on limited range correlation parameters. (Related to Fig. 1.)** I repeated the calculations from Fig. 1, in all cases for populations of 200 neurons. I repeated the calculations for different values of ρ_{max} and λ , the parameters that define the limited-range correlations. For each set of parameters, I computed the ratio of Fisher information in the full population of 200 neurons, vs. the Fisher information in just the tuned subset of (70% of) the population. Error bars are the S.E.M. over 10 random sets of different tuning curves.

526

Information-limiting correlations and Fig. S2

527

I repeated the calculations from Fig. 3, using the same random tuning curve shapes (as in Fig. 1A), but different covariance matrices. (In both Figs. S2A and S2B, the neurons had Poisson-like variability, as is seen experimentally). In Fig. S2A, the neurons had the *differential correlations* studied by [19, 23]. These correlations are such that the shared (correlated) part of the population noise mimics the changes in neural firing pattern induced by changes in the stimulus, thereby causing the distributions of responses to different stimuli to overlap substantially. As a result of that overlap in the stimulus-evoked response distributions, the noise substantially hinders the population code, and thus information saturates with increasing population size.

533

That covariance matrix, C_A , is given by

534

$$C_A(s) = C_o + \Upsilon \vec{f}'(s) \vec{f}'^T(s), \quad (8)$$

535

where Υ is a (small) scalar parameter that sets the strength of the differential correlations, and C_o is a diagonal matrix with entries equal to the mean firing rates given by $f(s)$. For $\Upsilon = 0$, this covariance matrix describes independent neurons with Poisson variability. For the results in Fig. S2A, I chose $\Upsilon = 5 \times 10^{-3}$, corresponding to weak but non-zero differential correlations.

536

537

538

539

Because changes in the stimulus do not change the mean firing rates of the untuned neurons – and the differential correlations mean the correlated noise mimics the stimulus-evoked changes in firing rates – the untuned neurons are unaffected by the correlated noise. This means that, with “pure” differential correlations, the noise in the untuned neurons is independent from the noise in the tuned ones. Consequently, ignoring the untuned neurons causes no loss of information (Fig. S2A: full population and tuned subset have the same information values).

540

541

542

543

544

545

To consider a case with information-limiting correlations in the tuned population, but with correlations between the tuned and untuned cells, I modified the differential correlation structure such that the untuned

546

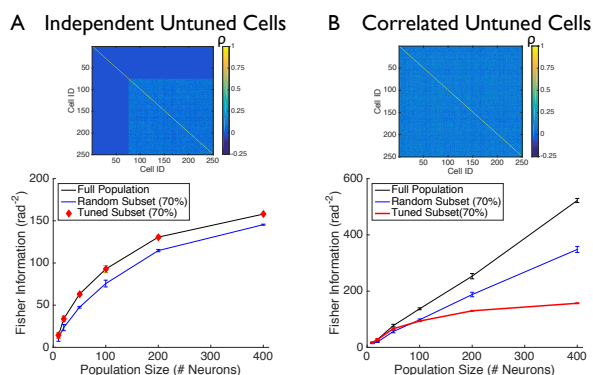
547
548
549

neurons were correlated with the tuned ones. Specifically, I modified Eq. 8 in a fashion that kept the tuned subset of the population unchanged, but made the untuned subset correlated with the tuned one. To do this, I used the formula

$$C_B(s) = C_o + \Upsilon \bar{g}(s) \bar{g}^T(s), \quad (9)$$

550
551
552
553

where $g_i(s) = f'_i(s)$ if the neuron is tuned, and $g_i(s) \sim \mathcal{N}(0, 5)$ if the neuron is untuned. If only the subset of tuned neurons is considered, $C_A = C_B$. For the untuned neurons, the corresponding rows and columns of C_A are all zeros, whereas for C_B , they are randomly generated non-zero values. Figure S2B used the same value of Υ as Fig. S2A.



Supplementary Figure 2: **Untuned neurons improve population coding when they are correlated with the tuned neurons. (Similar to Fig. 3, but with information-limiting correlations)** I considered neural populations with tuning curves as in Fig. 1, and where the untuned neurons were either independent of the tuned ones (A), or where the untuned neurons were correlated with the tuned ones (B). 70% of the neurons in each population were tuned to the stimulus, and 30% were untuned. Upper panels show correlation matrices for 250-cell populations: cells 1 through 75 are untuned, whereas the remainder were tuned. Center panels show the Fisher information for the full neural populations (black), for the tuned subsets of neurons (red), and for random subsets of 70% of the neurons in each population (blue). (Data points shown are mean \pm S.E.M., computed over 5 different random draws of the tuning curves).

554
555
556
557
558
559
560
561
562
563
564
565
566
567

For the tuned subset of the population, the noise structure in Fig. S2B was identical to the one in Fig. S2A (both contain differential correlations), and thus the tuned subsets of neurons have the same information in both cases. (Red data points in Fig. S2A have the same values as do points on the red curve in Fig. S2B). Different from Fig. S2A, the full population contained much more information than did the tuned subset, indicating that the untuned neurons do contribute to the population code in this case.

Thus, the observation that, when there are correlations between tuned and untuned neurons, untuned neurons improve population coding, holds in the case of information-limiting correlations (Fig. S2).

At the same time, it is important to note that the case of purely untuned neurons, with information-limiting correlations (Fig. S2), is, in some sense, pathological. Because the untuned neurons have no tuning, any noise that is correlated between the untuned and tuned cells will not perfectly match the stimulus-dependent changes in neural firing rates (i.e., the correlations will not be of the “pure” information-limiting type anymore, once correlations between tuned and untuned cells are included). Consequently, the large increase in information from including the untuned neurons seen in Fig. S2B will not occur if there is even weak tuning to the “untuned” population (because in that case, the “untuned” cells could be correlated with the strongly-tuned ones, while

568 maintaining a pure information-limiting correlation structure).

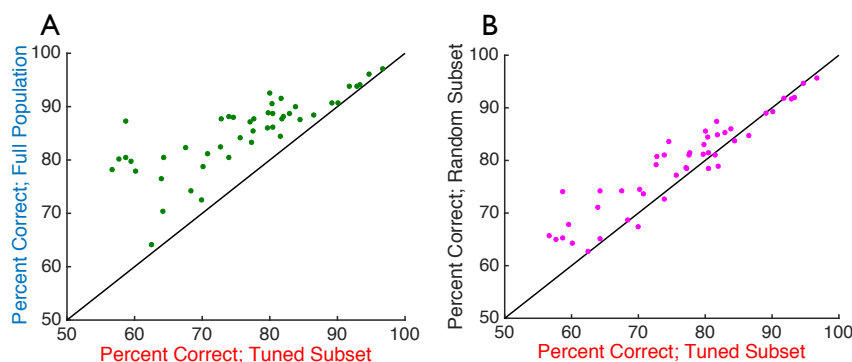
569 For this reason, we chose to focus the result in the main paper (Fig. 3) on a limited-range correlation
570 structure, which has no such pathology: Fig. 3 would be qualitatively unchanged if the “untuned” neurons were
571 made weakly tuned instead of perfectly untuned.

572 Varying the DSI cutoff for labelling cells as “tuned” vs “untuned”; Figs. S3 and S4

573 I repeated the analysis from Fig. 6 with two different cutoffs on the direction selectivity index (DSI), which is
574 used to distinguish “tuned” neurons from “untuned” ones.

575 DSI cutoff of 0.3 (Fig. S3):

576 I labeled cells with $DSI > 0.3$ as “tuned” and those with $DSI < 0.3$ as “untuned”. I then compared the
577 logistic regression decoding performance on the full population with that on the tuned subset of the population.
578 The full population yielded $13 \pm 2\%$ better decoding performance ($p = 4.7 \times 10^{-12}$, paired sample single-sided t
579 test; $p < 10^{-8}$, non-parametric binomial test of significance).



Supplementary Figure 3: **Untuned neurons can enhance information coding in *in vivo* neural populations.** (Similar to Fig. 6, but with a cutoff of $DSI > 0.3$ for labeling cells as “tuned”.) I used logistic regression to perform pairwise discrimination on the population response vectors, to determine which of 2 different stimuli caused each response. I repeated this analysis for all possible pairs of stimuli: reported values are the percentage of trials for which the stimulus was correctly identified, averaged over all possible pairings (there is one data point per experiment). (A) Decoding accuracy when the full population response vectors were decoded (vertical axis) vs. when only the tuned subsets of the neurons are seen by the decoder (horizontal axis). (B) Decoding accuracy when random subsets of the neurons (of the same size as the tuned subset, but containing both tuned and untuned neurons) are input to the decoder (vertical axis) vs. when only the tuned subsets of the neurons are seen by the decoder (horizontal axis). Chance performance for this binary discrimination task is 50%. Diagonal line denotes equality.

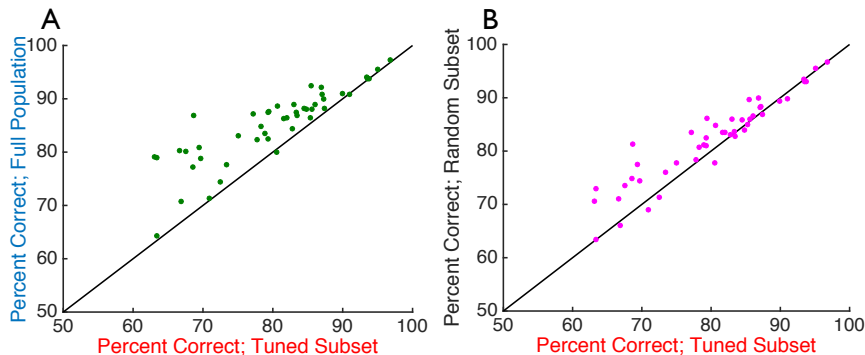
580 Next, I asked whether populations that include both tuned and untuned neurons could yield better decoding vs
581 populations of the same size but containing only tuned cells. To answer this question, I extracted a random subset
582 of the neurons from each population, that was the same size as the set of tuned neurons within that population.
583 I then performed the logistic regression analysis on these random subsets, and compared the performance with
584 that which was obtained on the tuned subsets. On average, the decoding performance was $5 \pm 1\%$ (mean \pm

585
586
587
588
589
590
591

S.E.M.) better using the random subsets vs the fully tuned ones, a modest but statistically significant difference ($p = 3.9 \times 10^{-6}$, paired single-sided t-test; and $p = 2.2 \times 10^{-3}$, non-parametric binomial test of significance).

DSI cutoff of 0.2 (Fig. S4):

I labeled cells with $DSI > 0.2$ as “tuned” and those with $DSI < 0.2$ as “untuned”. I then compared the logistic regression decoding performance on the full population with that on the tuned subset of the population. The full population yielded $7 \pm 1\%$ better decoding performance ($p = 9.8 \times 10^{-10}$, paired sample single-sided t test; $p < 10^{-8}$, non-parametric binomial test of significance).



Supplementary Figure 4: **Untuned neurons can enhance information coding in *in vivo* neural populations.** (Similar to Fig. 6, but with a cutoff of $DSI > 0.2$ for labeling cells as “tuned”.) I used logistic regression to perform pairwise discrimination on the population response vectors, to determine which of 2 different stimuli caused each response. I repeated this analysis for all possible pairs of stimuli: reported values are the percentage of trials for which the stimulus was correctly identified, averaged over all possible pairings (there is one data point per experiment). (A) Decoding accuracy when the full population response vectors were decoded (vertical axis) vs. when only the tuned subsets of the neurons are seen by the decoder (horizontal axis). (B) Decoding accuracy when random subsets of the neurons (of the same size as the tuned subset, but containing both tuned and untuned neurons) are input to the decoder (vertical axis) vs. when only the tuned subsets of the neurons are seen by the decoder (horizontal axis). Chance performance for this binary discrimination task is 50%. Diagonal line denotes equality.

592
593
594
595
596
597
598

Next, I asked whether populations that include both tuned and untuned neurons could yield better decoding vs populations of the same size but containing only tuned cells. To answer this question, I extracted a random subset of the neurons from each population, that was the same size as the set of tuned neurons within that population. I then performed the logistic regression analysis on these random subsets, and compared the performance with that which was obtained on the tuned subsets. On average, the decoding performance was $3 \pm 1\%$ (mean \pm S.E.M.) better using the random subsets vs the fully tuned ones, a modest but statistically significant difference ($p = 2.7 \times 10^{-5}$, paired single-sided t-test; and $p = 5.7 \times 10^{-3}$, non-parametric binomial test of significance).